



Grid dependence of RANS codes for flows past propeller blade sections

David Hally

Defence R&D Canada – Atlantic

Technical Memorandum
DRDC Atlantic TM 2008-262
April 2009

This page intentionally left blank.

Grid dependence of RANS codes for flows past propeller blade sections

David Hally

Defence R&D Canada – Atlantic

Technical Memorandum

DRDC Atlantic TM 2008-262

April 2009

Principal Author

Original signed by David Hally

David Hally

Approved by

Original signed by D. Hopkin

D. Hopkin
Head/Maritime Asset Protection

Approved for release by

Original signed by Ron Kuwahara for

C. Hyatt
Head/Document Review Panel

ANSYS® and CFX® are registered trademarks of ANSYS, Inc. or its subsidiaries in the United States or other countries.

CFX® is a trademark of Sony Corporation in Japan.

Pointwise® is a registered trademark and Pointwise Glyph™ is a trademark of Pointwise Inc.

© Her Majesty the Queen in Right of Canada as represented by the Minister of National Defence, 2009

© Sa Majesté la Reine (en droit du Canada), telle que représentée par le ministre de la Défense nationale, 2009

Abstract

The grid sensitivity of the Reynolds-averaged Navier-Stokes (RANS) solvers ANSYS CFX (ANSYS, Inc.) and TRANSOM (DRDC Atlantic) has been tested for two-dimensional flows around propeller blade sections. This is a preliminary step before developing grids for the solution of flows around cavitating propellers. The sensitivity of the pressure and skin friction distributions near the leading edge were tested for variations in near wall node spacing, the node density near the leading edge, and the overall size of the grid.

Résumé

La sensibilité du maillage des solutionneurs de l'Analyse d'équations de Navier-Stokes moyennées (RANS) ANSYS CFX (ANSYS, Inc.) et de TRANSOM (RDDC Atlantique) a été éprouvée pour les écoulements bi-dimensionnels autour de sections de pales d'hélice. Il s'agit d'une étape préliminaire avant l'élaboration de maillages pour la solution des écoulements autour des hélices avec cavitation. La sensibilité des distributions de pression et de résistance de friction près du bord d'attaque ont été éprouvées en vue de déceler les variations dans l'espacement de nœud près des parois, la densité de nœud près du bord d'attaque et les dimensions hors-tout du maillage.

This page intentionally left blank.

Executive summary

Grid dependence of RANS codes for flows past propeller blade sections

David Hally; DRDC Atlantic TM 2008-262; Defence R&D Canada – Atlantic; April 2009.

Background: The Maritime Asset Protection Section at DRDC Atlantic is applying Reynolds-averaged Navier-Stokes (RANS) solvers to the prediction of the flow around propellers so that the noise generated by propeller cavitation can be predicted. An important part of this research effort is to determine how best to generate the computational grids around the propeller. Since propeller blades are made from a series of airfoil-shaped sections, as a preliminary step, the grid sensitivity of two-dimensional RANS calculations around propeller blade sections was addressed first.

Principal results: The sensitivity of the RANS solvers ANSYS CFX (ANSYS, Inc.) and TRANSOM (DRDC Atlantic) to variations in computational grids has been assessed for flows around propeller blade sections. The sensitivity of the pressure and skin friction distributions near the leading edge were tested for variations in near wall node spacing, the node density near the leading edge, and the overall size of the grid.

Significance of results: These calculations provide information on how computational grids on propellers should be constructed so that accurate predictions of the pressures distribution can be obtained. This is a preliminary step in an attempt to calculate the flow over full propellers so that cavitation, and ultimately radiated noise levels, can be predicted.

Future work: Procedures for generating grids on propellers will be developed. The grids will be used with ANSYS CFX and TRANSOM to calculate flows past propellers for which good experimental data are available. Once accurate predictions of the flow are attained, procedures for calculating the propeller cavitation will be developed and used to develop a radiated noise model.

Sommaire

Grid dependence of RANS codes for flows past propeller blade sections

David Hally ; DRDC Atlantic TM 2008-262 ; R & D pour la défense Canada – Atlantique ; avril 2009.

Contexte : La section de Protection des biens maritimes de RDDC Atlantique applique les solutionneurs de l'Analyse d'équations de Navier-Stokes moyennées (RANS) à la prédiction de l'écoulement autour des hélices afin de pouvoir prédire le bruit produit par la cavitation de l'hélice. Cet effort de recherche vise, en grande partie, à déterminer comment produire les meilleurs maillages informatiques autour de l'hélice. Puisque les pales d'hélices sont fabriquées d'une série de sections en forme de profil aérodynamique, en tant qu'étape préliminaire, la sensibilité de maillage des calculs RANS bi-dimensionnels autour des sections de pales d'hélice a été abordée en premier.

Résultats : La sensibilité des solutionneurs RANS ANSYS CFX (ANSYS, Inc.) et TRANSOM (RDDC Atlantique) aux variations des maillages informatiques a été évaluée pour les écoulements autour de sections de pales d'hélice. La sensibilité des distributions de pression et de résistance de friction près du bord d'attaque a été éprouvée en vue de déceler les variations dans l'espacement de nœud près des parois, la densité de nœud près du bord d'attaque et les dimensions hors-tout du maillage.

Importance : Ces calculs fournissent de l'information sur la façon dont les maillages informatiques sur les hélices doivent être fabriquées afin de pouvoir obtenir des prédictions précises de la distribution des pressions. Il s'agit d'une étape préliminaire dans une tentative de calcul de l'écoulement sur des hélices complètes de façon à pouvoir calculer les niveaux de bruit de cavitation et, à la limite, de bruit rayonné.

Perspectives : Des méthodes de production de maillages sur hélices seront élaborées. Les maillages seront utilisés avec l'ANSYS CFX et TRANSOM pour calculer les écoulements sur les hélices pour lesquels de bonnes données expérimentales sont déjà disponibles. Une fois que des prédictions précises de l'écoulement seront obtenues, des méthodes pour le calcul de la cavitation d'hélice seront élaborées et utilisées pour le développement d'un modèle de bruit rayonné.

Table of contents

| | |
|---|-----|
| Abstract | i |
| Résumé | i |
| Executive summary | iii |
| Sommaire | iv |
| Table of contents | v |
| List of figures | vi |
| 1 Introduction | 1 |
| 2 Procedure for making grids in Pointwise | 1 |
| 2.1 The TRANSOM grid | 2 |
| 2.2 The grid for ANSYS CFX | 4 |
| 3 Sensitivity to grid parameters | 5 |
| 3.1 Sensitivity to wall spacing | 6 |
| 3.2 Sensitivity to node spacing at the leading edge | 8 |
| 3.3 Sensitivity to the size of the grid | 10 |
| 3.4 Sensitivity of ANSYS CFX to the size of the elements near the outer boundary | 11 |
| 3.5 Sensitivity of ANSYS CFX to the turbulence intensity | 11 |
| 4 Predictions of maximum pressure | 12 |
| 5 Concluding remarks | 12 |
| References | 14 |
| List of symbols | 15 |

List of figures

| | | |
|------------|---|----|
| Figure 1: | A trailing edge before (left) and after (right) closure with a semi-circular extension (right). | 2 |
| Figure 2: | An example of a grid used by TRANSOM. | 3 |
| Figure 3: | An example of a grid generated for ANSYS CFX. | 5 |
| Figure 4: | The DTMB modified NACA 66 airfoil with zero camber and thickness to chord ratio of 0.06. | 5 |
| Figure 5: | Pressure coefficient near the leading edge at different values of s ; ANSYS CFX on the left, TRANSOM on the right. | 6 |
| Figure 6: | Skin friction coefficient near the leading edge at different values of s ; ANSYS CFX on the left, TRANSOM on the right. | 7 |
| Figure 7: | Comparison of ANSYS CFX and TRANSOM predictions of the pressure coefficient near the leading edge with $s = 1$ | 7 |
| Figure 8: | Comparison of ANSYS CFX and TRANSOM predictions of the skin friction coefficient near the leading edge with $s = 0.5$ | 7 |
| Figure 9: | Variation of lift (left) and drag (right) coefficients with y^+ | 8 |
| Figure 10: | Nodes near the leading edge when $N_{le} = 3$ | 9 |
| Figure 11: | Pressure coefficient near the leading edge at different values of N_{le} | 9 |
| Figure 12: | Skin friction coefficient near the leading edge at different values of N_{le} | 9 |
| Figure 13: | Pressure coefficient near the leading edge for different grid sizes. | 10 |
| Figure 14: | Skin friction coefficient near the leading edge for different grid sizes. | 10 |
| Figure 15: | Skin friction coefficient near the leading edge for different levels of turbulence in the free stream. | 11 |
| Figure 16: | Cavitation buckets for the DTMB modified NACA 66 airfoil with 2% camber ratio as calculated by TRANSOM and ANSYS CFX. | 13 |

1 Introduction

The Maritime Asset Protection Section at DRDC Atlantic wishes to apply Reynolds-averaged Navier-Stokes (RANS) solvers to the prediction of cavitation on marine propellers. One question of interest is how dense the grid must be on the blade surface in order to model the pressure adequately. The answer will have important implications for the gridding strategy used. Since over most of a propeller blade the flow can be approximated by two-dimensional flow over a series of airfoil-shaped sections, the simpler question of the required grid density for airfoils was tackled first.

The DTMB modification [1] to the NACA 66 airfoil was used for this study. It has often been used as a section for propellers.

A series of grids were generated using the grid generator Pointwise [2]. Scripts were written using the Pointwise scripting language Pointwise Glyph (based on the programming language Tcl) to allow the automatic generation of grids suitable for use with the RANS solvers currently used by DRDC Atlantic: ANSYS CFX [3], a commercial code from ANSYS, Inc.; and TRANSOM, a code developed at DRDC Atlantic [4]. Each grid depends on a number of parameters which were then varied to determine their effects on the pressure and skin-friction distributions. Particular importance was placed on the flow near the leading edge where cavitation will normally appear.

It is important to note that this study was neither a verification nor a validation exercise. There are no comparisons with experiment, nor with theoretical solutions. Both ANSYS CFX and TRANSOM have been validated extensively [5,6]. It is merely a study to determine what grid density is necessary to produce results that do not depend on the grid.

2 Procedure for making grids in Pointwise

Two scripts were written in Pointwise Glyph: one to generate grids for ANSYS CFX and the other to generate grids for TRANSOM. Each starts with the geometry of the airfoil in IGES [7] format.

An O-topology was chosen for the grids as this is the topology planned for gridding propellers. The trailing edge of the airfoil is closed using a nearly semi-circular extension: see [Figure 1](#). This makes it easier to implement the O-topology. On a propeller, a similar closure at the trailing edge causes the whole propeller blade to be smooth with no mismatch at the tip between a smooth leading edge and sharp trailing edge.

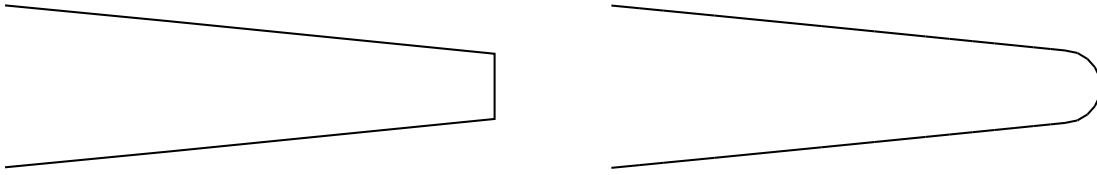


Figure 1: A trailing edge before (left) and after (right) closure with a semi-circular extension (right).

2.1 The TRANSOM grid

The TRANSOM grid is structured and uses O-topology. It is generated by extrusion from the airfoil surface. The grid is controlled by six parameters each of which is given a nominal value. The parameters, with their nominal values in brackets (all distances are relative to the chord length), are:

1. The mean spacing of the nodes on the airfoil (0.02).
2. The number of nodes per radius of curvature at the leading edge ($N_{le} = 5$).
3. The number of nodes per radius of curvature at the trailing edge ($N_{te} = 5$).
4. The node spacing between nodes on the airfoil and those just off it (10^{-5}).
5. The rate at which node spacing grows close to the airfoil (1.1).
6. The approximate outer radius of the grid ($R = 20$).

The grid is constructed as follows:

1. The spacing of the nodes at the leading edge and the trailing edge is determined according to the values of N_{le} and N_{te} and the thickness of the airfoil. (The leading edge radius of curvature varies as the square of the thickness, the trailing edge curvature in proportion to the thickness.)
2. The node spacing at the leading edge is allowed to increase geometrically by a factor of 1.1 until the spacing between nodes is equal to the mean spacing. This requires

$$N = \left\lceil \frac{\log(s_m/s_{te})}{\log(1.1)} \right\rceil + 2 \quad (1)$$

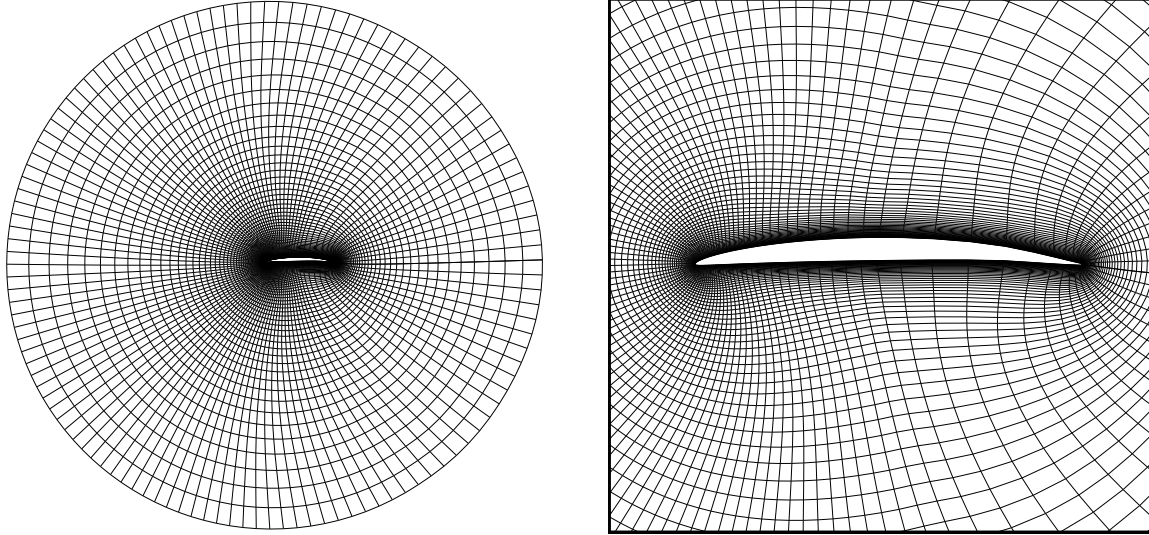


Figure 2: An example of a grid used by TRANSOM. The full grid is shown on the left, a close-up near the airfoil on the right. This grid is coarser near the leading and trailing edges than the grids actually used.

nodes on each side of the leading edge, where s_m is the mean spacing, s_{le} is the spacing at the leading edge and $|x|$ denotes the closest integer to x .

3. The nodes near the trailing edge are handled in a similar fashion to those at the leading edge.
4. The remainder of the airfoil is covered by nodes whose spacing is the mean spacing.
5. The nodes at the airfoil surface are extruded for N_e steps using the Pointwise hyperbolic extrusion with

$$N_e = \left\lceil \frac{\log(1 + R(w - 1)/s_w)}{\log(w)} \right\rceil \quad (2)$$

where R is the outer radius, w is the extrusion growth rate and s_w is the node separation at the wall. A Kinsey-Barth smoothing factor of 3 is used during the extrusion.

6. The grid is saved in PLOT3D format.

An example of a TRANSOM grid is shown in [Figure 2](#).

2.2 The grid for ANSYS CFX

The grids used with ANSYS CFX are hybrid with an inner structured block with O-topology and an outer unstructured block. The outer boundary is a square (this simplifies the setting of boundary conditions in the ANSYS CFX pre-processor). The inner block is generated by extrusion from the airfoil surface. The grid is controlled by nine parameters each of which is given a nominal value. The parameters, with their nominal values in brackets (all distances are relative to the chord length), are:

1. The mean spacing of the nodes on the airfoil (0.02).
2. The number of nodes per radius of curvature at the leading edge ($N_{le} = 5$).
3. The number of nodes per radius of curvature at the trailing edge ($N_{te} = 5$).
4. The node spacing between nodes on the airfoil and those just off it (10^{-5}).
5. The rate at which node spacing grows close to the airfoil (1.1).
6. The distance to extrude the inner block (0.1).
7. The half-length of a side of the outer square boundary ($R = 20$). (We choose the half-length so that it is comparable to the radius of the TRANSOM grid.)
8. The node spacing on the outer square boundary (2).
9. The boundary decay factor for the unstructured outer domain. Values near 1 mean that the cell sizes change less rapidly (0.99).

The grid is constructed as follows:

1. Generate the inner domain as if making a TRANSOM grid, but only extrude over the size of the inner grid.
2. Make four edges to form the square outer boundary and populate them with nodes using the appropriate spacing.
3. Generate an unstructured domain between the outer boundary and the outer edge of the inner domain using the specified boundary decay factor.
4. Use translational extrusion to convert the two-dimensional grid into a three-dimensional grid two cells deep (ANSYS CFX requires a three-dimensional grid).
5. Set boundary conditions on each exterior domain.
6. Save the grid in ANSYS CFX format.

An example of a grid for ANSYS CFX is shown in [Figure 3](#).

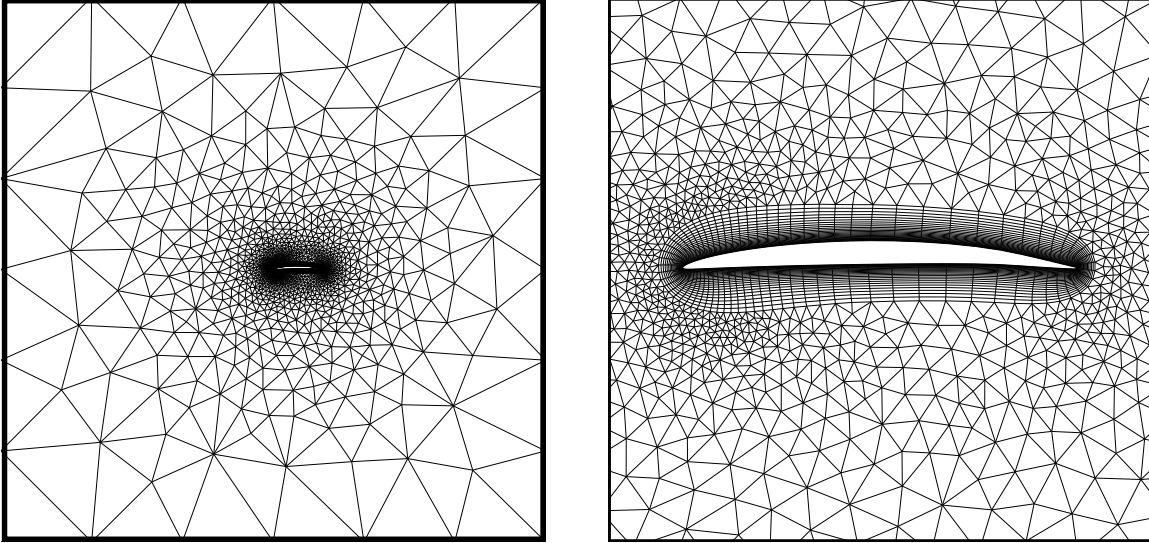


Figure 3: An example of a grid generated for ANSYS CFX. The full grid is shown on the left, a close-up near the airfoil on the right. This grid is coarser near the leading and trailing edges than the grids actually used.

NACA 66 (DTMB mod): $t = 0.06$ $c = 0$

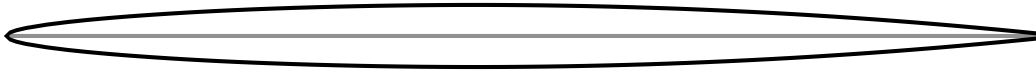


Figure 4: The DTMB modified NACA 66 airfoil with zero camber and thickness to chord ratio of 0.06.

3 Sensitivity to grid parameters

The study of sensitivity to grid parameters used the DTMB modified NACA 66 airfoil with thickness to chord ratio of 0.06, roughly typical of a section about halfway up a propeller blade, and with no camber: see [Figure 4](#).

The flow past the airfoil was calculated at an angle of attack of 4° , large enough to generate a significant pressure peak with a value of the pressure coefficient, C_p , near -6 . For all calculations the Reynolds number based on the airfoil chord was $Re = 10^7$. For the calculations with ANSYS CFX the SST turbulence model [8] was used, while for TRANSOM the Spalart-Allmaras turbulence model [9] was used.

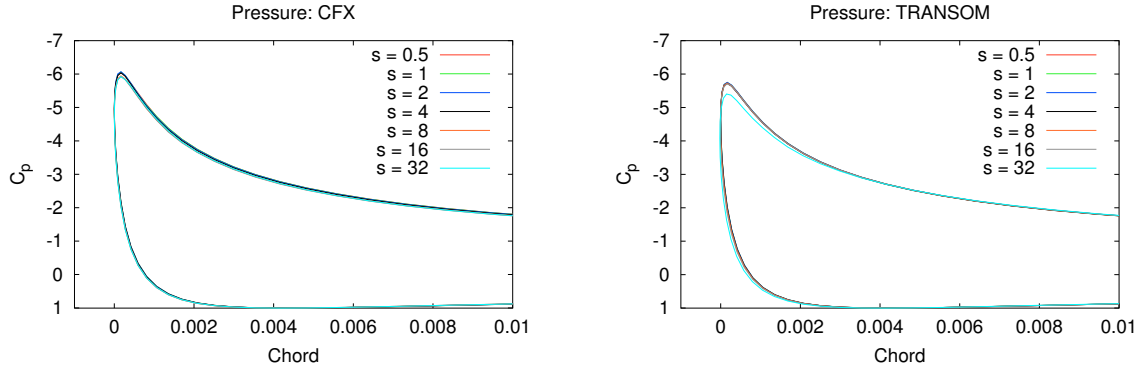


Figure 5: Pressure coefficient near the leading edge at different values of s ; ANSYS CFX on the left, TRANSOM on the right.

3.1 Sensitivity to wall spacing

The separation of the wall from the nodes closest to it is usually measured using the parameter y^+ :

$$y^+ \equiv \frac{u^* y}{\nu}; \quad u^{*2} \equiv \nu \frac{\partial v}{\partial y} \quad (3)$$

where ν is the kinematic viscosity, v is the component of the velocity parallel to the wall and y is the distance to the wall. Because the value of y^+ depends on the velocity, it has a peak near the leading edge where both the velocity and pressure have peaks. Therefore the values of y^+ near the pressure peak can be quite high relative to the values over the main portion of the airfoil. Is it necessary to choose the wall-spacing based on the high values of y^+ in the pressure peak?

The wall spacing for the initial grid generated for ANSYS CFX was chosen so that the largest value of y^+ was about 11. The ANSYS CFX scalable wall functions effectively set the minimum allowed value of y^+ to 11, so we expect to see little change if the wall spacing is smaller than this. A series of grids were then generated in which the wall spacing was smaller or larger than the initial value by a factor, s . A similar procedure was used for the TRANSOM grids except that the wall spacing of the initial grid was set so that the largest value of y^+ was 1 (TRANSOM does not use wall functions so the nodes must be closer to the wall than for ANSYS CFX). Thus, if $s = 2$, the largest value of y^+ for the grid generated for ANSYS CFX is about 22, while for the TRANSOM grid it is about 2. The value $s = 1$ represents a wall spacing that, a priori, would be considered optimal.

For both solvers the spacing of the nodes at the leading edge was set so that $N_{le} = 10$.

Figure 5 shows the pressure coefficient predicted by both solvers near the leading edge as a function of the chordwise distance (the leading edge is 0; the trailing edge

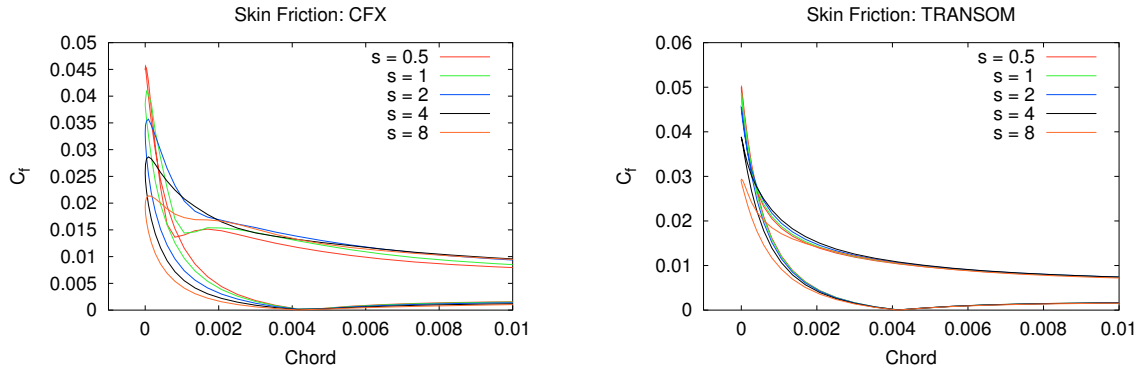


Figure 6: Skin friction coefficient near the leading edge at different values of s ; ANSYS CFX on the left, TRANSOM on the right.

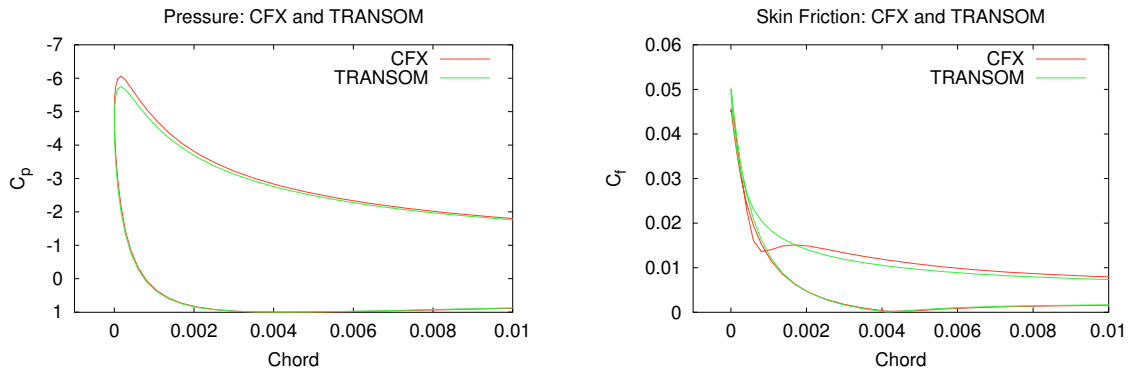


Figure 7: Comparison of ANSYS CFX and TRANSOM predictions of the pressure coefficient near the leading edge with $s = 1$.

Figure 8: Comparison of ANSYS CFX and TRANSOM predictions of the skin friction coefficient near the leading edge with $s = 0.5$.

is 1). The ANSYS CFX predictions vary very little for y^+ as high as 350, while the TRANSOM predictions are just beginning to degenerate when y^+ reaches 32. Clearly the pressure is insensitive to the wall spacing. As the pressure distribution is almost entirely a potential flow effect, this is what should be expected.

Figure 6 shows the skin friction coefficient, C_f , near the leading edge. In this case there is a clear dependence on wall spacing for both ANSYS CFX and TRANSOM. With ANSYS CFX, the dependence continues even to spacings somewhat smaller than $s = 1$. The TRANSOM results have converged at $s = 1$ but begin to diverge for larger spacings.

Figure 7 compares the pressure and skin friction distributions when $s = 1$ predicted by ANSYS CFX and TRANSOM. There is very good agreement. Similarly, Figure 8 compares the skin friction distributions when $s = 0.5$. The agreement is good except

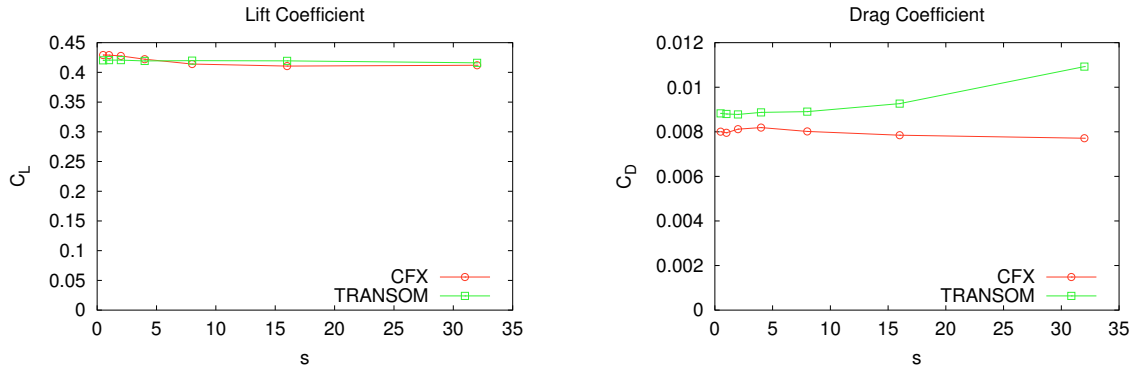


Figure 9: Variation of lift (left) and drag (right) coefficients with y^+ .

for a small region just aft of the pressure peak on the suction side where the ANSYS CFX prediction is smaller than that of TRANSOM. Therefore, as should be expected, when each solver is used with near-optimal node spacing, they produce very similar results.

It is important to note that when $s > 1$, the region over which the skin friction is not well predicted is very small; consequently, the effect on the lift and drag of the airfoil is also small: see Figure 9. Therefore, when gridding a propeller, it will be sufficient to choose the near wall spacing so that y^+ is close to 1 (TRANSOM) or 11 (ANSYS CFX) over the main portion of the airfoil; if it exceeds these values near the pressure peak, there will be little effect on the predicted propeller performance.

3.2 Sensitivity to node spacing at the leading edge

To test the sensitivity to the spacing of the nodes near the leading edge, grids were generated for which N_{le} , the number of nodes within one leading edge radius of curvature, was 3, 5, 10, 15 or 20. Since the radius of curvature at the leading edge is 1.63×10^{-3} , these value of N_{le} correspond to node spacings of 5.43×10^{-4} , 3.26×10^{-4} , 1.63×10^{-4} , 1.09×10^{-4} and 8.15×10^{-5} . Figure 10 shows the nodes near the leading edge (the same for both ANSYS CFX and TRANSOM grids) when N_{le} is 3.

In all cases the wall spacing was chosen so that y^+ has a maximum value of 1 for TRANSOM and 11 for ANSYS CFX.

Figure 11 shows the pressure coefficient near the leading edge as a function of the chordwise distance. For both ANSYS CFX and TRANSOM the pressure is well-predicted at $N_{le} = 5$. There is only a small change in the pressure peak when N_{le} is reduced to 3.

Figure 12 shows the skin friction coefficient, C_f , near the leading edge. In this case

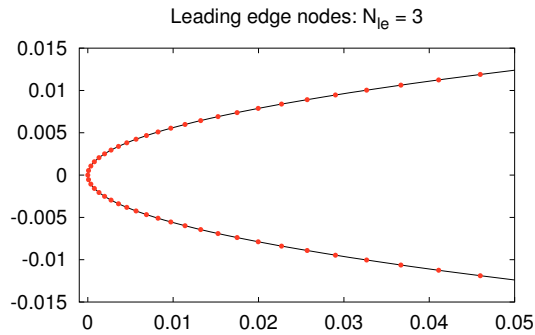


Figure 10: Nodes near the leading edge when $N_{le} = 3$.

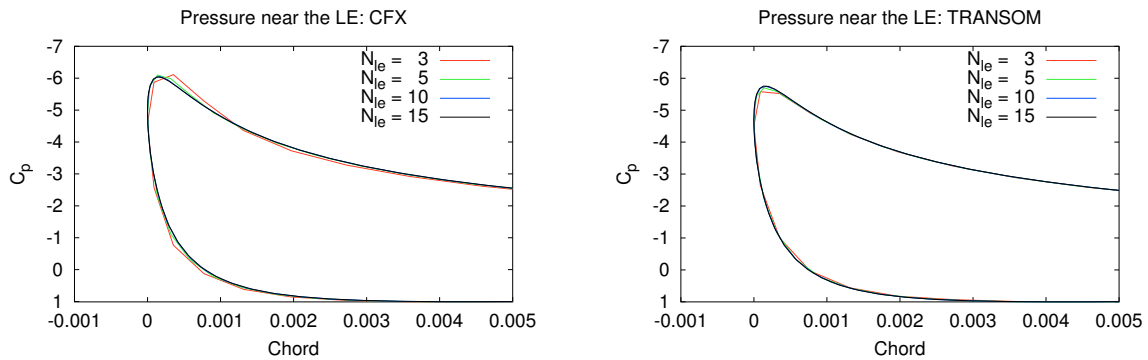


Figure 11: Pressure coefficient near the leading edge at different values of N_{le} , the number of nodes relative to the radius of curvature leading edge; ANSYS CFX on the left, TRANSOM on the right.

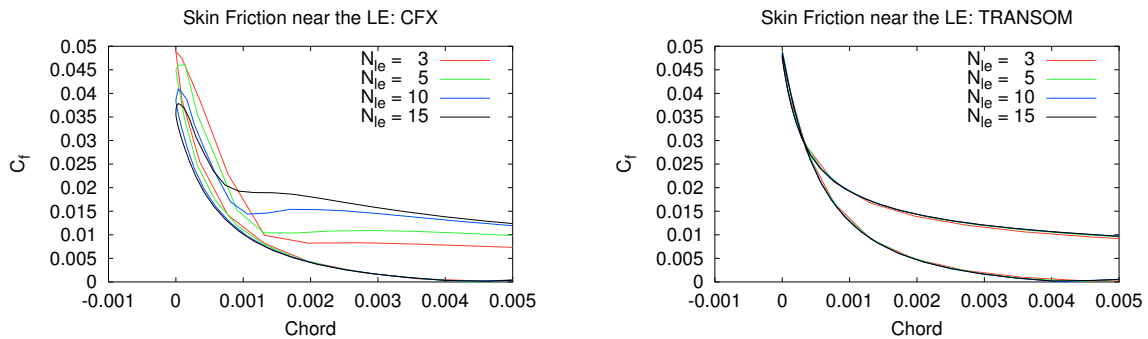


Figure 12: Skin friction coefficient near the leading edge at different values of N_{le} , the number of nodes relative to the radius of curvature leading edge; ANSYS CFX on the left, TRANSOM on the right.

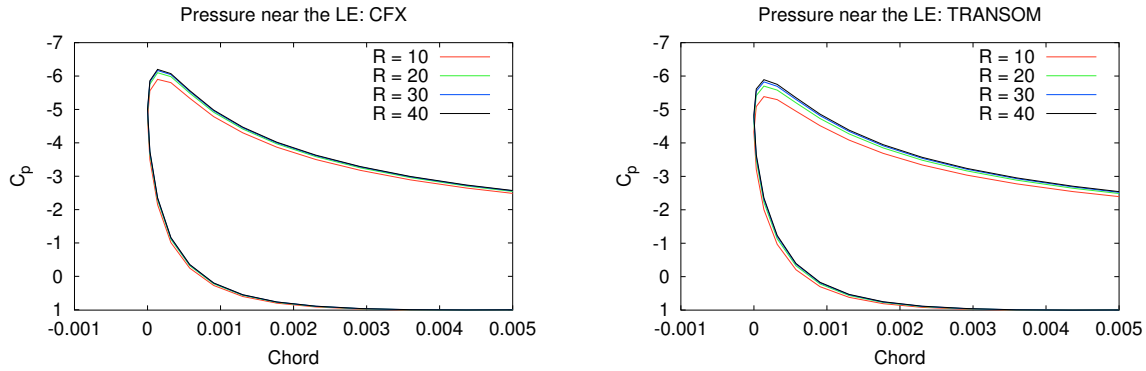


Figure 13: Pressure coefficient near the leading edge for different grid sizes; ANSYS CFX on the left, TRANSOM on the right.

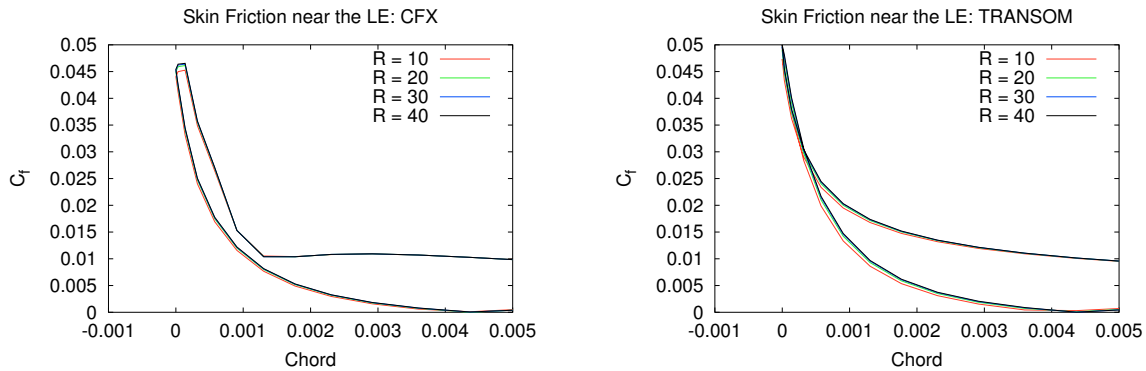


Figure 14: Skin friction coefficient near the leading edge for different grid sizes; ANSYS CFX on the left, TRANSOM on the right.

the ANSYS CFX predictions show a clear dependence on N_{le} , though not enough to alter the lift or drag significantly. The TRANSOM results are nearly independent of N_{le} .

3.3 Sensitivity to the size of the grid

To test the sensitivity to the overall size of the grid, R , grids were generated for which R was 10, 20, 30 or 40. In all cases the wall spacing was chosen so that y^+ has a maximum value of 1 for TRANSOM and 11 for ANSYS CFX. For both solvers the spacing of the nodes at the leading edge was set so that $N_{le} = 10$.

Figure 13 shows the pressure coefficient near the leading edge as a function of the chordwise distance. For both ANSYS CFX and TRANSOM there is little variation with R , the largest deviation occurring, as expected, when $R = 10$. Figure 14 shows that the skin-friction coefficient near the leading edge is likewise insensitive to R .

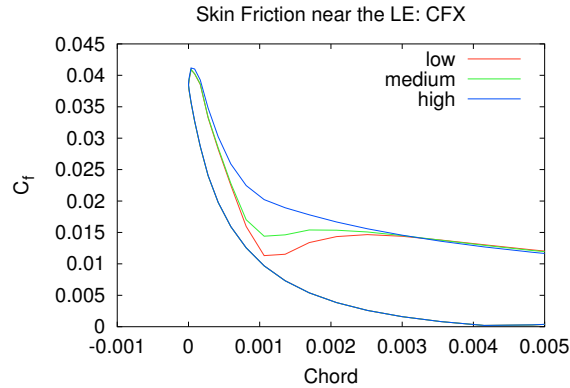


Figure 15: Skin friction coefficient near the leading edge for different levels of turbulence in the free stream.

3.4 Sensitivity of ANSYS CFX to the size of the elements near the outer boundary

To test the sensitivity to the overall size of the grid, R , grids were generated for which the outer node spacing was 0.5, 1, 2 or 3. The effect on the pressure distribution and the skin-friction distribution was so small as to be indiscernible when plotted.

3.5 Sensitivity of ANSYS CFX to the turbulence intensity

At inlet boundaries, ANSYS CFX requires that the values of turbulence variables be set. This sets the level of turbulence in the free stream. In all the runs described here this was done by specifying the turbulence intensity, I , and the viscosity ratio μ_t/μ . Three preset options are provided called low ($I = 1\%$, $\mu_t/\mu = 1$), medium ($I = 5\%$, $\mu_t/\mu = 10$) and high ($I = 10\%$, $\mu_t/\mu = 100$). The effect of these settings on the skin friction coefficient near the leading edge is shown in [Figure 15](#).

The level of turbulence has a clear effect on the skin friction just aft of the pressure peak on the suction side of the blade, the region where there was a difference between ANSYS CFX and TRANSOM. Once again, the difference is not sufficiently large that there will be an appreciable effect on the lift or drag.

The level of turbulence had no discernible effect on the pressure distribution.

4 Predictions of maximum pressure

To put the size of the variations with the grid parameters into perspective relative to the variations one finds between solvers, the maximum pressure on a series of airfoils was calculated for different cambers, thicknesses and angles of attack using both ANSYS CFX and TRANSOM. The results for the DTMB modified NACA 66 airfoil with camber of 2% of chord are plotted as cavitation buckets in [Figure 16](#). Each curve shows the relationship between the angle of attack and the minimum value of the pressure coefficient, C_p , on the airfoil. The different curves represent different thickness to camber ratios.

Relative to TRANSOM, ANSYS CFX tends to predict slightly higher peak pressures for positive angles of attack, slightly lower for negative angles of attack. This results in a small upward shift of the buckets relative to those predicted by TRANSOM. The same effect can be seen in [Figure 7](#). The reason for this discrepancy is not understood. The effect exceeds the effects shown by variations in the grid (for example, compare [Figures 5 and 11](#) with [Figure 7](#)), so it is believed to be caused by the inherent differences in the solvers.

When the thickness $t = 0.02$ the TRANSOM curve shows the minimum pressure dropping precipitously once the angle of attack gets too large. This is due to separation beginning near the leading edge causing the airfoil to stall. The lack of similar behaviour in the ANSYS CFX shows that the airfoil has not yet stalled even at significantly larger angles of attack. This discrepancy is almost certainly due to the different turbulence models used: SST for ANSYS CFX and Spalart-Allmaras for TRANSOM.

These results suggest that errors associated with grids constructed using the nominal parameters given in [Sections 2.1 and 2.2](#) will be smaller than the modelling errors associated with the different solvers and turbulence models.

5 Concluding remarks

The grid sensitivity of the RANS solvers ANSYS CFX and TRANSOM has been assessed for two-dimensional flows around propeller blade sections at small angles of attack. Both solvers show little sensitivity to the grid parameters tested. These results suggest that accurate predictions of the leading edge pressure peaks on propeller blades can be attained with ANSYS CFX provided that the y^+ values of the near wall nodes is within the log-layer of the boundary layer ($y^+ \lesssim 300$) and the leading edge node density is such that at least five nodes are contained within one radius of curvature. The distance to the outer boundary of the grid should exceed 10 chord lengths. Similarly, TRANSOM will require y^+ values not exceeding about 16. It is not so clear whether these restrictions will be adequate to predict the complicated vortex production near the propeller tip.

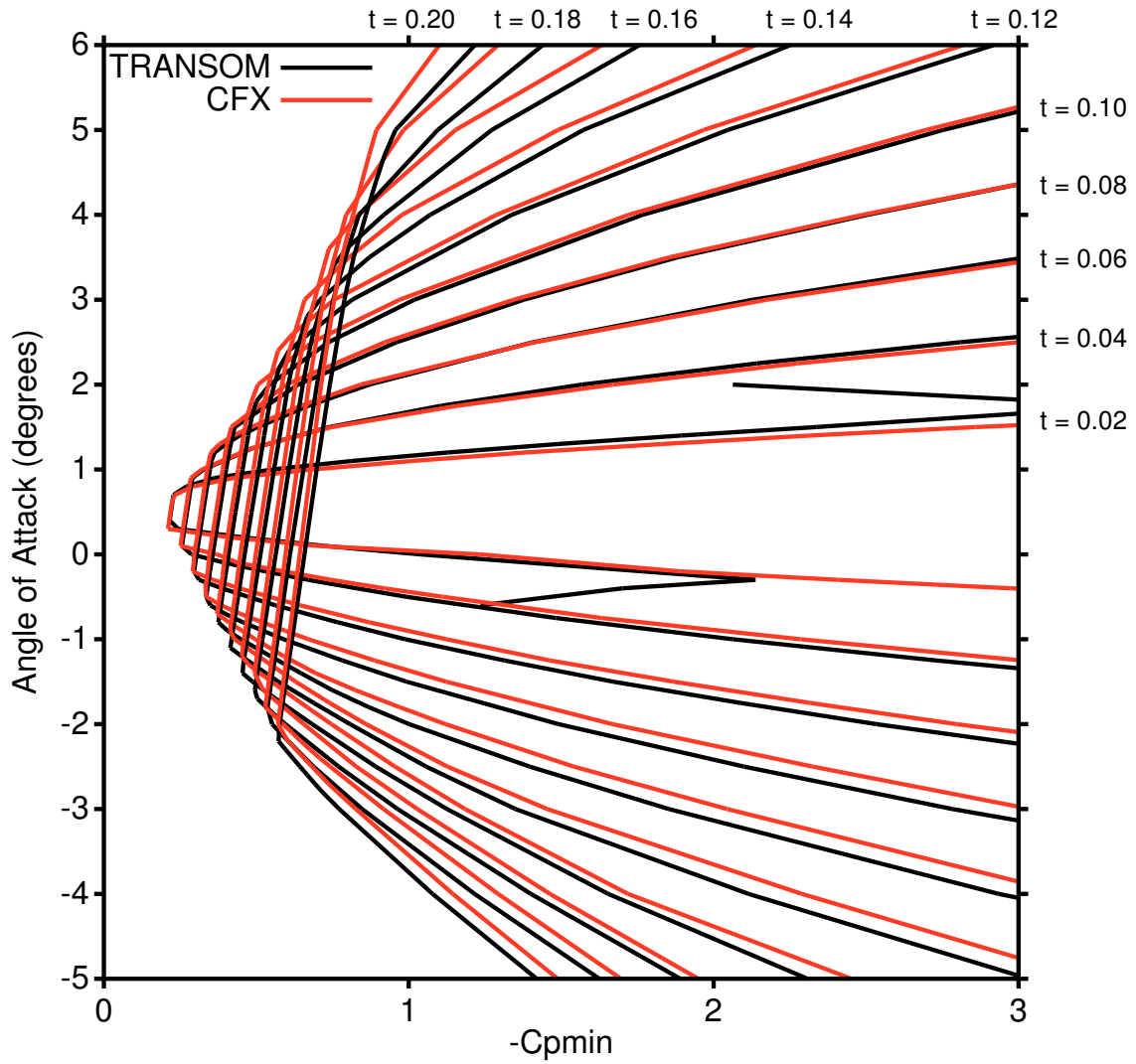


Figure 16: Cavitation buckets for the DTMB modified NACA 66 airfoil with 2% camber ratio as calculated by TRANSOM and ANSYS CFX.

References

- [1] Brockett, T. (1966), Minimum Pressure Envelopes for Modified NACA-66 Sections with NACA $a = 0.8$ Camber and BuShips Type I and Type II Sections, (Report 1780) David W. Taylor Naval Ship Research and Development Center.
- [2] (2008), Pointwise: Reliable CFD Meshing You Trust (online), Pointwise, Inc., Fort Worth, Texas, <http://www.pointwise.com> (Access Date: November 2008).
- [3] (2008), ANSYS CFX (online), ANSYS, Inc., <http://www.ansys.com/products/cfx.asp> (Access Date: November 2008).
- [4] Hally, D. (1997), TRANSOM: A Multi-method Navier-Stokes Solver: Overall Design, (DREA TM 97-231) Defence R&D Canada – Atlantic.
- [5] Hally, D. (2001), TRANSOM calculations of the flow past SSPA 720, (DREA TR 2001-167) Defence R&D Canada – Atlantic.
- [6] Chisholm, T. and Zingg, D. W. (2005), Validation of TRANSOM, (DRDC Atlantic CR 2004-229) Defence R&D Canada – Atlantic.
- [7] (1988), Initial Graphics Exchange Specification (IGES) Version 4.0, US Dept. of Commerce, National Bureau of Standards. Document No. NBSIR 88-3813.
- [8] Menter, F. R. (1993), Zonal Two Equation $k-\omega$ Turbulence Models for Aerodynamic Flows, Technical Report AIAA Paper 93-2906.
- [9] Spalart, P. R. and Allmaras, S. R. (1992), A One-Equation Turbulence Model for Aerodynamic Flows, Technical Report AIAA Paper 92-0439.

List of symbols

- μ Viscosity.
- μ_t Eddy viscosity.
- ν Kinematic viscosity.
- C_f The skin friction coefficient.
- C_p The pressure coefficient.
- I Turbulence intensity.
- N_{le} The number of nodes per radius of curvature at the leading edge.
- N_{te} The number of nodes per radius of curvature at the leading edge.
- R The outer radius of a TRANSOM grid. The half length of the outer square of a grid used by ANSYS CFX.
- s A factor used to indicate the relative spacing of the near-wall nodes in different grids.
- s_{le} Spacing of the nodes on the airfoil surface at the leading edge.
- s_m Mean spacing of the nodes on the airfoil surface.
- s_w The spacing between nodes on the airfoil and those just off it.
- t Thickness to chord ratio of an airfoil.
- u^* Shear velocity: see [Equation \(3\)](#).
- w The growth rate of the extrusion of the structured block.
- y^+ Non-dimensional distance to the airfoil surface: see [Equation \(3\)](#).

This page intentionally left blank.

Distribution list

DRDC Atlantic TM 2008-262

Internal distribution

- 1 Author
- 3 Library

Total internal copies: 4

External distribution

Department of National Defence

- 1 DRDKIM
- 2 DMSS 2

Others

- 1 Library and Archives Canada
395 Wellington Street
Ottawa, Ontario
K1A 0N4
Attn: Military Archivist, Government Records Branch
- 1 Director-General
Institute for Marine Dynamics
National Research Council of Canada
P.O. Box 12093, Station A
St. John's, Newfoundland
A1B 3T5
- 1 Director-General
Institute for Aerospace Research
National Research Council of Canada
Building M-13A
Ottawa, Ontario
K1A 0R6

- 1 Transport Development Centre
Transport Canada
6th Floor
800 Rene Levesque Blvd, West
Montreal, Que.
H3B 1X9
Attn: Marine R&D Coordinator

- 1 Canadian Coast Guard
Ship Safety Branch
Canada Building, 11th Floor
344 Slater Street
Ottawa, Ontario
K1A 0N7
Att: Chief, Design and Construction

MOUs

- 6 Canadian Project Officer ABCA-02-01 (C/SCI, DRDC Atlantic – 3 paper copies, 3 PDF files on CDROM)

Total external copies: 14

Total copie: 18

DOCUMENT CONTROL DATA

(Security classification of title, body of abstract and indexing annotation must be entered when document is classified)

| | | | |
|--|--|---|--|
| 1. ORIGINATOR (The name and address of the organization preparing the document. Organizations for whom the document was prepared, e.g. Centre sponsoring a contractor's report, or tasking agency, are entered in section 8.) Defence R&D Canada – Atlantic PO Box 1012, Dartmouth NS B2Y 3Z7, Canada | | 2. SECURITY CLASSIFICATION (Overall security classification of the document including special warning terms if applicable.) UNCLASSIFIED | |
| 3. TITLE (The complete document title as indicated on the title page. Its classification should be indicated by the appropriate abbreviation (S, C or U) in parentheses after the title.) Grid dependence of RANS codes for flows past propeller blade sections | | | |
| 4. AUTHORS (Last name, followed by initials – ranks, titles, etc. not to be used.) Hally, D. | | | |
| 5. DATE OF PUBLICATION (Month and year of publication of document.) April 2009 | 6a. NO. OF PAGES (Total containing information. Include Annexes, Appendices, etc.) 28 | 6b. NO. OF REFS (Total cited in document.) 9 | |
| 7. DESCRIPTIVE NOTES (The category of the document, e.g. technical report, technical note or memorandum. If appropriate, enter the type of report, e.g. interim, progress, summary, annual or final. Give the inclusive dates when a specific reporting period is covered.) Technical Memorandum | | | |
| 8. SPONSORING ACTIVITY (The name of the department project office or laboratory sponsoring the research and development – include address.) Defence R&D Canada – Atlantic PO Box 1012, Dartmouth NS B2Y 3Z7, Canada | | | |
| 9a. PROJECT OR GRANT NO. (If appropriate, the applicable research and development project or grant number under which the document was written. Please specify whether project or grant.) Project 11cd23 | | 9b. CONTRACT NO. (If appropriate, the applicable number under which the document was written.) | |
| 10a. ORIGINATOR'S DOCUMENT NUMBER (The official document number by which the document is identified by the originating activity. This number must be unique to this document.) DRDC Atlantic TM 2008-262 | | 10b. OTHER DOCUMENT NO(s). (Any other numbers which may be assigned this document either by the originator or by the sponsor.) | |
| 11. DOCUMENT AVAILABILITY (Any limitations on further dissemination of the document, other than those imposed by security classification.) (X) Unlimited distribution () Defence departments and defence contractors; further distribution only as approved () Defence departments and Canadian defence contractors; further distribution only as approved () Government departments and agencies; further distribution only as approved () Defence departments; further distribution only as approved () Other (please specify): | | | |
| 12. DOCUMENT ANNOUNCEMENT (Any limitation to the bibliographic announcement of this document. This will normally correspond to the Document Availability (11). However, where further distribution (beyond the audience specified in (11)) is possible, a wider announcement audience may be selected.) | | | |

13. ABSTRACT (A brief and factual summary of the document. It may also appear elsewhere in the body of the document itself. It is highly desirable that the abstract of classified documents be unclassified. Each paragraph of the abstract shall begin with an indication of the security classification of the information in the paragraph (unless the document itself is unclassified) represented as (S), (C), or (U). It is not necessary to include here abstracts in both official languages unless the text is bilingual.)

The grid sensitivity of the Reynolds-averaged Navier-Stokes (RANS) solvers ANSYS CFX (ANSYS, Inc.) and TRANSOM (DRDC Atlantic) has been tested for two-dimensional flows around propeller blade sections. This is a preliminary step before developing grids for the solution of flows around cavitating propellers. The sensitivity of the pressure and skin friction distributions near the leading edge were tested for variations in near wall node spacing, the node density near the leading edge, and the overall size of the grid.

14. KEYWORDS, DESCRIPTORS or IDENTIFIERS (Technically meaningful terms or short phrases that characterize a document and could be helpful in cataloguing the document. They should be selected so that no security classification is required. Identifiers, such as equipment model designation, trade name, military project code name, geographic location may also be included. If possible keywords should be selected from a published thesaurus. e.g. Thesaurus of Engineering and Scientific Terms (TEST) and that thesaurus identified. If it is not possible to select indexing terms which are Unclassified, the classification of each should be indicated as with the title.)

Propellers
Airfoils
Fluid flow
SST turbulence model
Spalart-Allmaras turbulence model
Grid generation
TRANSOM
ANSYS CFX
Pointwise
Pointwise Glyph

This page intentionally left blank.

Defence R&D Canada

Canada's leader in defence
and National Security
Science and Technology

R & D pour la défense Canada

Chef de file au Canada en matière
de science et de technologie pour
la défense et la sécurité nationale



www.drdc-rddc.gc.ca